

Femtosecond laser micro-structuring of alumina ceramic

W. Perrie^{a,*}, A. Rushton^a, M. Gill^a, P. Fox^a, W. O’Neill^b

^aDepartment of Engineering, University of Liverpool, Brownlow Hill, Liverpool L69 3GH, UK

^bInstitute For Manufacturing, Department of Engineering, University of Cambridge, Mill Lane, Cambridge CB2 11RX, UK

Available online 23 March 2005

Abstract

Al₂O₃ ceramic has been micro-structured in air using 180 fs, $\lambda = 775$ nm optical pulses in a fluence range $1.4 < F < 21$ J cm⁻² with observed ablation rates of $25 < V < 900$ $\mu\text{m}^3/\text{pulse}$. The threshold fluence was $F_{\text{th}} = 1.1$ J cm⁻² at this ultrashort pulse-length in the NIR. Melting could be minimised using ultrafast optical pulses, improving the edge quality. By optimising the processing parameters, the residual surface roughness could be reduced below the pristine surface $R_a = 0.8$ μm . The debris produced consists mainly of single crystal nanoparticles of alumina with diameters from 20 nm to 1 μm with an average diameter of 300 nm.

© 2005 Elsevier B.V. All rights reserved.

PACS: 79.20.D; 42.62.C

Keywords: Femtosecond laser ablation; Micro-machining; Alumina; Re-deposition

1. Introduction

Ceramic alumina (Al₂O₃) is an important substrate used in hybrid circuits due to its high dielectric strength coupled with an excellent thermal stability and high thermal conductivity of 25 W m⁻¹ K⁻¹. As conventional mechanical punching and stamping in these substrates becomes limited below dimensions of a few hundred micrometers, laser processing offers potential advantages including the elimination of tool wear.

A detailed study of the characteristics of nanosecond and femtosecond excimer UV ablation of oxide ceramics, including alumina was carried out by Ihlemann et al. [1,2]. Using time resolved absorption measurements of the sample and the ablation plume, they demonstrated that nanosecond UV ablation is “plasma mediated” while the coupling of femtosecond UV radiation at $\lambda = 248$ nm is dominated by two-photon absorption (TPA), negating thermal effects, allowing micrometer level surface structuring. Under nanosecond UV pulses, incubation of defects leads to a strong increase in the bulk absorption coefficient. The release of electrons in the first few nanoseconds leads to avalanche breakdown of the surface. The rest

* Corresponding author. Tel.: +44 151794 4918;
fax: +44 151794 4675.

E-mail address: wpfemto1@liv.ac.uk (W. Perrie).

of the incoming pulse couples strongly with the developing plasma, which also ablates the material.

NIR single and multi-pulse sub-picosecond and picosecond ablation of sapphire (Al_2O_3) at $\lambda = 790$ nm (0.2–5 ps) shows that 0.2 ps multi-pulse micro-structuring is superior to that at 2.3 and 4.5 ps, eliminating surface cracks [3]. Ablation characteristics showed two phases. A gentle ablation phase for low pulse number, with typical ablation rate of 40 nm/pulse, followed by an explosive phase with ablation rate 10 times higher and consistent with a six photon process. Single pulse and multi-pulse fluence thresholds with pulselength of $0.2 < \tau_p < 4.5$ ps have also been measured, yielding multi-pulse fluence thresholds of 1.3 J cm^{-2} for 0.2 ps and increasing to 3.6 J cm^{-2} at 4.5 ps [4]. Time-of-flight mass spectrometry during femtosecond ablation of sapphire at 790 nm [5] produced only Al^+ , O^+ and O^{2+} ions with high kinetic energies of $E \sim 100$ eV which support a Coulomb explosion mechanism at the surface. The observed ion energy increase with the pulse number indicates that incubation of defects on sapphire during femtosecond ablation is also important.

Femtosecond UV laser (0.5 ps, $\lambda = 248$ nm), used for micro-machining of another ceramic composite, Al_2O_3 –34 wt% TiC [6], has shown that at a low fluence of $F < 3 \text{ J cm}^{-2}$, a globular structure develops and the selective ablation of TiC leads to a significant increase of the surface roughness. Minimising the differential ablation of the two compounds was achieved at a high fluence of $F = 12 \text{ J cm}^{-2}$ with only a slight increase in surface roughness. Also, sub-micrometer patterning was demonstrated. In contrast, with nanosecond $\lambda = 248$ nm radiation, the roughness R_a was observed to increase with the fluence [7] and also a significant surface melting occurred resulting in a globular structure. Similar results were obtained on this composite for the excimer laser wavelength $\lambda = 308$ nm [8]. More recent nanosecond UV ablation studies of surface micro-structure and chemistry on alumina at $\lambda = 248$ nm also demonstrated the advantage of using a higher fluence for minimising melting and improving the surface roughness [9]. Micro-cracks nevertheless could not be avoided and a $< 1 \mu\text{m}$ thick re-melted surface layer was created on top of the surface.

The availability of femtosecond laser systems operating in the NIR with several milliJoule pulse

energies and kilohertz repetition rates provides currently convenient tools for micro-structuring of materials like metals and transparent dielectrics [10,11]. Also, at ultrahigh intensity ($I > 10^{12} \text{ W cm}^{-2}$), multi-photon absorption (MPA) yields an effective coupling mechanism to materials by using ultrashort optical pulses in the UV, visible or NIR.

In this work, we have studied micro-machining of alumina ceramic in air at 1 kHz repetition rate with energetic, $\lambda = 775$ nm, 180 fs optical pulses for optimising the processing conditions. Residual surface features, the ablation rate and the residual surface roughness were determined by interferometric microscopy (WYKO NT3300 surface profilometer) and scanning electron microscopy (SEM, Hitachi S-2450). The nature of the ablation debris was investigated with SEM and TEM (Jeol FX-1000).

2. Experimental details

The experimental set-up has been described in greater detail previously [12]. Briefly, the 1 kHz output from a Clark-CPA 2010 femtosecond laser was attenuated before directing it into a Scanning Galvo system with f -theta lens of focal length $f = 100$ mm, AR coated for $\lambda = 775$ nm. The focussed waist diameter ($1/e^2$) was $\sim 30 \mu\text{m}$. Machining patterns were controlled by software (SCAPS GmbH). The alumina substrates type AD-96 (Coors-Tek) had dimensions of $50 \text{ mm} \times 30 \text{ mm} \times 1 \text{ mm}$. They were located on the surface of a horizontally positioned mirror mount, supported on a mechanical vertical high resolution laboratory jack with $10 \mu\text{m}$ resolution.

3. Results and discussion

For our system, the energy deposited per unit area per second (average power density, W cm^{-2}) on the material surface during the focussed spot scan is given approximately by, $\langle I \rangle = \nu E_p / [(\varphi s t) + \pi \varphi^2 / 4]$, where $t = 1$ s, $\nu = 10^3$ Hz, E_p the pulse energy (J), φ the spot diameter (3×10^{-3} cm) and s is the scan speed (cm s^{-1}). This parameter gives an indication of the residual thermal effects, which can lead to detrimental micro-machining. Since the scan speed is $0.1 \leq s \leq 1 \text{ cm s}^{-1}$ while $10 \leq E_p \leq 150 \mu\text{J}$, $\langle I \rangle$ varies

in the range $3.3\text{--}500\text{ W cm}^{-2}$. There is a remarkable change in the ablation characteristics, i.e. the obtained surface relief and texture as $\langle I \rangle$ is varied in this range. High $\langle I \rangle \sim 300\text{ W cm}^{-2}$ is characterised by a significant surface re-deposition, melting and re-solidification. By reducing $\langle I \rangle$ to $\leq 50\text{ W cm}^{-2}$, micro-structuring improves markedly, see Fig. 1a–c. Fig. 1a shows a SEM image of surface machining for $\langle I \rangle = 6.7\text{ W cm}^{-2}$ with good edge definition. Around the walls, and at the base of the machined area, the original micro-structure is strongly modified, possibly due to melting and successive re-solidification of alumina during laser processing. In Fig. 1b, which shows the base at higher magnification, the morphology shows sub-micrometer pores consistent with the creation of a thin amorphous layer. This thin layer was

observed at $\langle I \rangle = 3.3\text{ W cm}^{-2}$ by fracturing a laser treated area to give a cross-section through the surface (Fig. 1c). This SEM image shows a $\sim 2\text{ }\mu\text{m}$ thick surface layer of lower porosity sitting on top of the crystalline ceramic, consistent with rapid re-melting. This layer thickness is essentially independent of the machined depth. However, there are no signs of micro-cracks, as observed during nanosecond UV structuring [9].

The nature of debris generated at $\langle I \rangle = 16.5\text{ W cm}^{-2}$ was investigated by collecting it on a TEM grid placed close to an ablation spot (Fig. 1d). The TEM image shows that the debris consists mainly of spherical nanoparticles with a wide range of diameters from 10 nm to $\sim 1\text{ }\mu\text{m}$, with an average diameter of 300 nm . Electron diffraction shows these

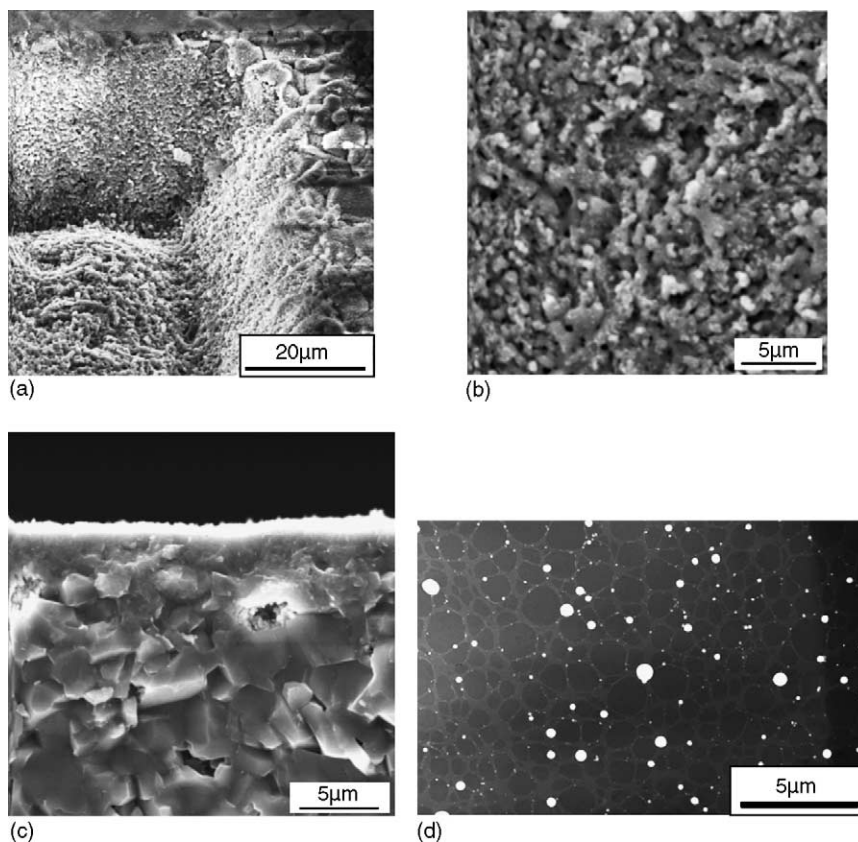


Fig. 1. (a) SEM image of alumina micro-structuring ($\sim 20\text{ }\mu\text{m}$ depth) at a fluence of $F = 2.8\text{ J cm}^{-2}$ and average scanned intensity $\langle I \rangle = 6.7\text{ W cm}^{-2}$. (b) Detail of micro-structured surface of the sample in (a) showing random structures on the melted surface. (c) SEM image of a cross-section through the processed alumina surface machined at a fluence $F = 1.4\text{ J cm}^{-2}$ and low scanned intensity $\langle I \rangle = 3.3\text{ W cm}^{-2}$. A $2\text{ }\mu\text{m}$ thick modified layer is observed. (d) TEM image of typical debris for NIR femtosecond ablation of alumina showing spherical particles with $20\text{ nm--}1\text{ }\mu\text{m}$ diameter, generated at $\langle I \rangle = 16.5\text{ W cm}^{-2}$.

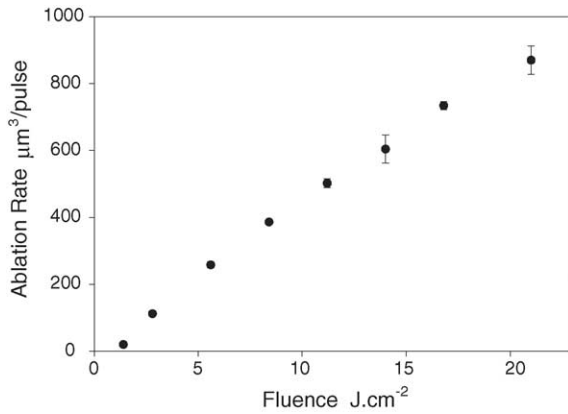


Fig. 2. Measured ablation rate vs. fluence for alumina laser processed at $\lambda = 775$ nm, 180 fs. Error bars represent $\pm\sigma$.

particles to be essentially single crystalline, probably formed by rapid cooling and condensation of the resulting plasma behind the shock front [13,14].

A series of 200 μm wide tracks were machined at $s = 10$ mm s^{-1} , 10 μm hatch with identical scanning geometry while varying the pulse energy. The resulting track profiles and depths, which were measured using the WYKO optical surface profiler allowed the calculation of femtosecond ablation rates. Fig. 2 shows the observed ablation rate ($\mu m^3/pulse$) of alumina as a function of fluence. At a fluence of $F = 21.5$ $J \cdot cm^{-2}$, the volume ablation rate of ~ 900 $\mu m^3/pulse$ corresponds to an ablation depth of $d = 1.3$ $\mu m/pulse$. Fig. 3 shows how the measured

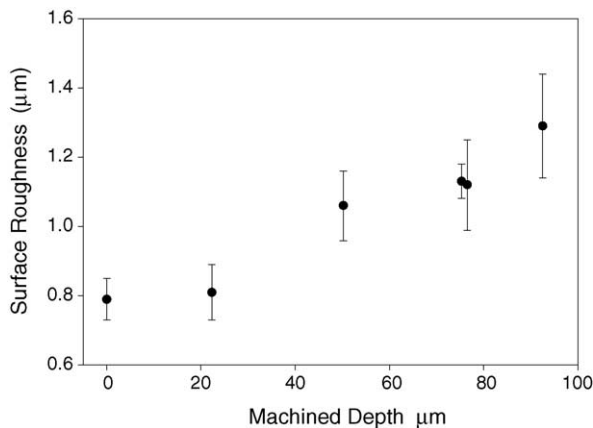


Fig. 3. Measured surface roughness with machined depth at fluence of $F = 2.8$ $J \cdot cm^{-2}$, $\langle I \rangle = 6.7$ $W \cdot cm^{-2}$. Error bars represent $\pm\sigma$.

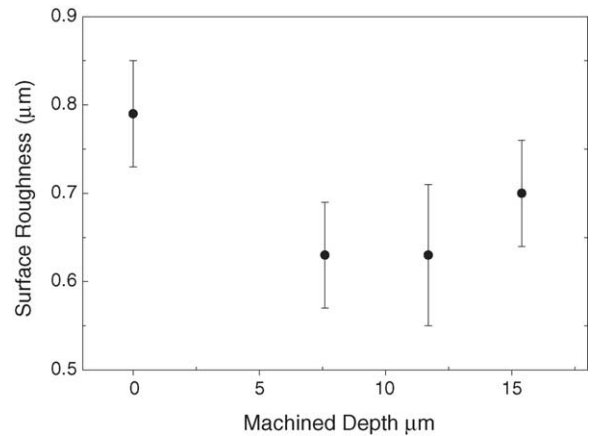


Fig. 4. Observed surface roughness with depth at a fluence of $F = 1.4$ $J \cdot cm^{-2}$, $\langle I \rangle = 3.3$ $W \cdot cm^{-2}$ showing that surface roughness can be reduced slightly below a depth of 15 μm . Error bars represent $\pm\sigma$.

residual surface roughness R_a increases with machined depth when fluence $F = 2.8$ $J \cdot cm^{-2}$. The growth of the surface roughness with depth arises partly due to debris re-deposition, which affects the developing surface relief. However, when the fluence was reduced to $F = 1.4$ $J \cdot cm^{-2}$, just above ablation threshold, the machined surface showed a slight decrease of the roughness to a depth of about 15 μm (Fig. 4). The threshold fluence was estimated by the observation of the onset of a very weak surface plasma under low background light, yielding $F_{th} \sim 1.1$ $J \cdot cm^{-2}$.

4. Conclusions

Femtosecond NIR optical pulses have been used to micro-structure ceramic alumina with excellent edge quality observed at low scanned intensities ≤ 50 $W \cdot cm^{-2}$. The treated surface exhibits no discoloration, unlike that produced by nanosecond UV processing at $\lambda = 248$ nm [9]. The pristine surface roughness $R_a = 0.79 \pm 0.07$ μm can be reduced slightly by using a pulse fluence of $F = 1.4$ $J \cdot cm^{-2}$, while a surface roughness increase up to depths of ~ 150 μm was obtained with scanned intensity $\langle I \rangle$ in the range 7–50 $W \cdot cm^{-2}$. A ~ 2 μm thick re-melted layer occurs on the surface by the NIR femtosecond processing of alumina. The ablation threshold (multi-pulse) of $F = 1.1$ $J \cdot cm^{-2}$ found here for alumina is close to that observed for sapphire with $\lambda = 790$ nm at

0.2 ps [4], which is not surprising since alumina is poly-crystalline sapphire. The use of low scanned intensity $<10 \text{ W cm}^{-2}$ minimises the material re-deposition and surface roughness and residual thermal effects which cause melting and re-solidification.

Acknowledgments

We would like to thank our technical staff in the Department of Engineering, in particular, Mr. Lawrence Bailey and Mr. Richard Arnold.

References

- [1] J. Ihlemann, A. Scholl, H. Schmidt, B. Wolff-Rottke, *Appl. Phys. A60* (1995) 411.
- [2] J. Ihlemann, B. Wolff-Rottke, *Appl. Surf. Sci.* 106 (1996) 282.
- [3] D. Ashkenasi, A. Rosenfeld, H. Varel, M. Wahmer, E.E.B. Campbell, *Appl. Surf. Sci.* 120 (1997) 65.
- [4] D. Ashkenasi, R. Stoian, A. Rosenfeld, *Appl. Surf. Sci.* 154–155 (2000) 40.
- [5] H. Varel, M. Wahmer, A. Rosenfeld, D. Ashkenasi, E.E.B. Campbell, *Appl. Surf. Sci.* 127–129 (1998) 128.
- [6] M. Mendes, V. Oliveira, R. Vilar, *J. Las. Appl.* 11 (5) (1999) 211.
- [7] V. Oliveira, R. Vilar, O. Conde, *Appl. Surf. Sci.* 127–129 (1998) 831.
- [8] M. Mendes, V. Oliveira, R. Vilar, F. Beinhorn, J. Ihlemann, O. Conde, *Appl. Surf. Sci.* 154–155 (2000) 29.
- [9] D. Sciti, C. Melandri, A. Bellosi, *J. Mat. Sci.* 35 (2000) 3799.
- [10] N.H. Rizvi, *RIKEN Review*, No. 50, 2003.
- [11] D. Ashkenasi, G. Muller, A. Rosenfeld, R. Stoian, I.V. Hertel, N.M. Bulgakova, E.E.B. Campbell, *Appl. Phys. A77* (2003) 223.
- [12] W. Perrie, M. Gill, G. Robinson, P. Fox, W. O'Neill, *Appl. Surf. Sci.* 230 (2004) 50.
- [13] M. Mendes, R. Vilar, *Appl. Surf. Sci.* 217 (2003) 149.
- [14] W. Marine, L. Patrone, B. Luk'yanchuck, M. Sentis, *Appl. Surf. Sci.* 154–155 (2000) 345.